DOI: 10.1134/S1027451020070022

STRESS DISTRIBUTIONS IN P91 MARTENSITIC STEEL AND IN AISI 316LN STEEL WELDS FOR GEN IV NUCLEAR APPLICATIONS

P. Agostini[1], G. Barbieri[2], R. Coppola [3]*, M. Moncada[2], C. Ohms [4], R. C. Wimpory[5]

[1] ENEA-Brasimone, FSN, CP 1, 40032 Camugnano (BO), Italy

[2] ENEA-Casaccia, SSTP-PROMAS-MATPRO, Via Anguillarese 301, 00123 Roma, Italy

[3] ENEA-Casaccia, FSN-SICNUC, Via Anguillarese 301, 00123 Roma, Italy

*e-mail: roberto.coppola@enea.it

[4] EU JRC, Petten, IET 1755ZG, The Netherlands
[5] HZB,Hahn-Meitner-Platz1,D-14109Berlin, Germany

Abstract – Neutron diffraction has been utilized to investigate the stress field in two different welds developed for nuclear applications, namely: a Tungsten Inert Gas (TIG) weld of P91 martensitic steel (Cr 9 Mn 6 Mo 1 C 0.1 Fe bal wt%) and a hybrid laser beam and gas metal arc weld (LB - GMAW) of AISI316LN austenitic steel (17.8 Cr, 12.3 Ni, 1.7 Mn, 2.4 Mo, 0.3 Si Fe bal wt%). The sizes of the investigated welded samples were 100 x 50 x 12 mm^3 for the P91 weld and 220 x 160 x 15 mm^3 for the 316LN weld; unstrained references were prepared for both welds. The neutron diffraction measurements have been carried out utilizing the E3 diffractometer at the BER II reactor in Berlin, with a gauge volume of 2x2x2 mm^3; lines perpendicular to the weld direction were scanned at different depths inside the material and at different distances from the weld center, including the heat affected zone (HAZ) and the weld center. Strain and stress values were determined in the three principal directions. In the TIG P91 weld the stresses are almost completely relieved after a post-weld heat treatment (PWHT) of 2 h at 760°C. In the LB - GMAW 316LN weld, not submitted to PWHT, nearly balancing longitudinal and transverse stress components as high as 300 – 350 MPa are found within a range of approximately 3 mm around the center of weld.

Keywords: neutron diffraction, stress measurements, nuclear welds

INTRODUCTION

The availability of advanced welding procedures constitutes a crucial pre-requisite in the development of safe and sustainable GEN IV reactors, where structural components including a large number of welds will be simultaneously exposed to high temperature, high neutron irradiation doses and aggressive environment [1-4]. In fact failure in metallic components occurs very often in and around welds, their integrity is therefore critical for the safe performance of nuclear components. It depends on a number of factors such as residual

stresses, mechanical properties of the weld, base material and heat affected zones (HAZ) as well as geometrical factors. The latter also depend on the basic material properties and on the welding process. Therefore it is clear that bulk characterization of nuclear welds is much more complicated than it is for base materials and that neutron diffraction is indispensable for such investigations [4-6].

This contribution presents experimental results obtained investigating by means of neutron diffraction the stress distributions present in two different model welds for nuclear application; these welds were produced in the frame of the European grant *MATTER: MATerials TEsting and Rules* [7], focused on the definition of experimental protocols for nuclear materials and components, and further characterized in the frame of European research program on nuclear materials *EERA JPNM: European Energy Research Alliance Joint Program Nuclear Materials* [8]. The first one, a P91 martensitic steel Tungsten Inert Gas (TIG) weld, has been selected from a series of similar welds prepared to systematically investigate the effectiveness of various post-weld heat treatments (PWHT) in reducing the residual stresses and improving the mechanical properties accordingly. The second weld, an AISI316LN austenitic steel hybrid laser beam and gas metal arc weld (LB - GMAW) has been prepared with the multiple aim of obtaining narrower HAZ's, reducing distortions and producing less severe thermal cycles with respect to conventional welding techniques. The two different steels were selected taking into account the different function of the respective welds, particularly the higher resistance of P91 steel to radiation damage. Both samples have been characterized by standard metallography, micro-hardness and mechanical testing [9, 10]. The neutron diffraction measurements were carried out to obtain bulk averaged residual stress distributions, necessary to contribute in predicting weld resistance to fatigue cracking and not obtainable by other experimental methods. It is emphasized that that the joint presentation of stress measurements obtained on two so different samples is not to be intended as a comparison between the two different welds and materials, but as two separate contributions provided by neutron diffraction to different milestones of the *MATTER* Project. It is also noted that the investigated welds are quite complex and, despite the standardization of the welding procedures, might exhibit micro-structural differences from one sample to another even for identical chemical composition and metallurgical treatments; therefore, the results presented here below are not intended as conclusive ones but as a first necessary step to understand the effectiveness of the adopted welding procedures in improving the nuclear components design.

SAMPLES CHARACTERIZATION AND EXPERIMENTAL TECHNIQUE

The chemical composition of the base metal in the investigated P91 martensitic steel TIG weld is the following: Cr 9, Mn 6, Mo 1, C 0.1, Fe bal wt%. The size of the investigated sample is 100 x 50 x 12 mm^3. It was welded by one pass TIG with 60° chamfer, then submitted to 2 h at 760°C PWHT. After heat treatment, a reduction of approximately 20% was observed in the micro-hardness (Fig. 1). The micro-structure of the as-welded base metal consists of prior-to-austenite grains containing a fine lath-like tempered martensite and varying with the distance from the weld center as shown in the optical micrography observations of Fig. 2. No significant micro-structural changes were detected after PWHT. In order to obtain an un-strained sample for base metal, HAZ and weld, a slice 6 mm thick was cut from the original weld with coupons eroded in correspondence of the points selected for the stress mapping: this comb-like sample is shown in Fig. 3. In this way, reference measurements were obtained for every location selected for stress measurements in the welded sample, in order to account as much as possible for possible variations in local chemistry and microstructure due to welding.

The chemical composition of the base metal in the investigated AISI 316LN austenitic steel LB – GMAW is the following: Cr 18, Ni 12, Mn 1.7, Mo 2. 4, C 0.03, Fe bal wt%. The size of the investigated sample is 220 x 160 x 15 mm^3; its transverse cross-section around the weld is shown in Fig. 4. Boheler Thermanit 19/15 was utilized as filler material. The weld was not submitted to any PWHT, consequently high stress gradients had to be expected close to the welded region. The weld was distorted by approximately 5.8°, as it shown in the cross-sectional picture of Fig. 5 (top). The comb-like reference sample with eroded coupons (Fig. 5 bottom) was obtained also in this case cutting a 6 mm thick slice from the welded sample.

Reference is made to [11] and to previous publications [12,13] for a description of strain and stress measurements by means of neutron and X-ray diffraction. The neutron diffraction measurements were carried out at room temperature utilizing the E3 diffractometer, installed at the BER II reactor [14]. A Si (400) monochromator was utilized providing a neutron wavelength λ= 1.47 Å. A diffracting volume of 2 x 2 x 2 mm^3 was selected to optimize counting time, metallurgical significance and benchmarking with future numerical simulations. For the bcc P91 martensitic steel weld the <211> reflection was exploited at a Bragg angle $2\theta \approx 78.8$. The <311> reflection of the fcc 316LN austenitic steel was

exploited, at a Bragg angle $2\theta \approx 85.5°$. The strains were measured in three independent directions namely longitudinal, transverse and normal with respect to the direction of the weld. For both samples, the reference comb-like sample was glued to the welded sample in correspondence of its original position: in this way a single positioning of welded and reference sample was sufficient to run the whole set of measurements, for each of the two investigated welds. The experimental uncertainty in peak position was in the range 0.003° - 0.006° approximately, corresponding to uncertainties of $3 – 6\ 10^{-5}$ for the strain values and typically ± 22 MPa for the stress values. The stresses were calculated assuming for the P91 steel a Young modulus E = 221 GPa and $\nu = 0.33$; for the 316LN steel E = 192 GPa and $\nu = 0.33$ were taken. For both the investigated welds, these E and ν values, referring to the base metals, were utilized also for determining the stresses in the HAZ and in the center of the weld.

EXPERIMENTAL RESULTS

An overview of the stress mapping obtained for the TIG P91 steel weld is shown in the 2D plots of Fig.s 6 a-c. These stress values have been obtained by measurements taken approximately 2 mm inside the welded samples, in the positions shown in Fig. 3, so that each eroded coupon could serve as a reference for the corresponding point inside the weld. For this ferritic P91 weld the reference variation over all measurements (parent and weld region) was 77.665° ±0.005° in 2θ which corresponds to ± 17 MPa. The peak width full width at half maximum (FWHM) increases by 11% in the weld region compared to the parent material. The 1D plot of Fig. 7 shows the stresses as a function of the distance from the weld center as measured along a line close to the weld cap; similar trends are found for 1D plots at different depths with respect to the weld cap. Very low stresses, comparable with the experimental uncertainty, are found homogeneously distributed throughout the weld. A measurement of the stresses in this same weld before PWHT would have been necessary to make a more general assessment; however, these results show that in the investigated sample after 2 h at 760°C the stress field is perfectly compatible with the engineering requirements and expected service conditions.

In the LB – GMAW 316LN sample, the stresses were determined in points at 11 different distances from the weld center and at 3 different heights from the weld root, both in the

straight and in the distorted side of weld and reference sample, correcting the positions for the 5.8° bending on the distorted side. The stresses were determined assuming zero longitudinal stresses in the reference sample and zero normal stresses in the welded sample: the agreement of the corresponding reference values is good, implying that such assumptions are correct. In fact the reference sample was a slice cut perpendicular to the weld longitudinal direction. It is expected that the out of plane stress in the slice (weld longitudinal direction) will be very low, close to zero and so a zero normal stress could be assumed. Similarly the actual weld has the shortest dimension in the weld normal direction, being geometrically a plate. The normal stress is typically very small, close to zero in this direction in this type of geometrical configuration. The variation in the austenitic 316LN weld reference was typically 85.450° ± 0.007° in the parent region in 2θ which corresponds to ± 19 MPa. The reference value was very different in the weld region, typically around 85.18° in 2θ. The peak width FWHM increases around 15% in the weld region compared to the parent region.

The results are shown in Fig.s 8 a-c, referring to the stress profiles as measured at the weld cap, in the middle length and at the weld bottom respectively. The measurements were affected by some additional uncertainty due to a grainy micro-structure inside the weld, which is the reason for some higher values of the error bars. It is anyhow clear that in the absence of a suitable PWHT the more innovative welding procedure applied to this steel can produce complex and relatively high stress distributions, particularly in the mid-thickness line (Fig. 8 b), with longitudinal tensile stresses as high as 300 MPa partly compensated by transverse compression.

DISCUSSION AND CONCLUSIONS

The obtained results show once more the capability of neutron diffraction to provide bulk averaged stress distributions in complex welds, including the HAZ and the center of the weld. In fact, uncertainties relating to metallurgical phase inhomogeneity in these regions are strongly reduced by the method selected for preparing comb-like reference samples perfectly coinciding with the original weld, as described in section 2. A more detailed investigation of such critical regions, HAZ and weld center, would require a resolution in the Bragg peaks

significantly higher than the one available for such experiments, in order to attempt a profile analysis and obtain information on phase changes as a function of depth inside the weld.

These results provide a useful contribution to the development of protocols for nuclear welds. Namely, the P91 TIG welds were designed to be as stress-free as possible and this is now confirmed at least for the case of the investigated sample. The stress distributions obtained for the LB - GMAW will help in adjusting the parameters of the welding procedure in view of improving the welding quality and expected performance in service. Clearly, a larger number of samples, for each of the two model welds, should be investigated to get wider and more general information. Other micro-structural investigations by destructive or semi-destructive techniques (transmission electron microscopy, small punch test, contour method) are currently in progress to complete the characterization of these welds and compare with the neutron diffraction results. Numerical simulations of the stress distributions will also be carried out to compare with the experimental ones.

ACKNOWLEDGMENTS

The Helmholtz Zentrum Berlin is gratefully acknowledged for beam-time allocation, technical assistance and travelling support. The research leading to these results has been carried out in the frame of EERA Joint Programme on Nuclear Materials and is partly funded by the European Commission HORIZON 2020 Framework Programme under grant agreement No. 755269. Dr. M. Valli (ENEA) is acknowledged for help in handling the P91 weld data.

REFERENCES

1) B. Hayes, Eng. Fail. Analysis, 3 (1996) 157-170 https://doi.org/10.1016/1350-6307(96)00015-5
2) D. Smith, P. Bouchard, D. George, J. of Strain Analysis for Eng. Des. 35 (2000) 287 – 305 DOI: 10.1243/0309324001514422
3) K. Kang and L. Kupca Ed.s, *Integrity of Reactor Pressure Vessel Steels in Nuclear Power Plants: Assessment of Irradiation Embrittlement in Reactor Pressure Vessel*

Steels, n. NP-T-3.11 in IAEA Nuclear Energy Series, Vienna, Austria, 2009, ISBN 978-92-0-101709-3

4) G. D. Bokuchava, P.Petrov, I. V. Papushkin, J. Surface Invest., 10, 6 (2016) 1143 - 1153 DOI: 10.1134/S1027451016050463

5) C. Ohms, R.V. Martins, O. Uca, A.G. Youtsos, P.J. Bouchard, M. Smith, M. Keavey, S.K. Bate, P. Gilles, R.C. Wimpory, L. Edwards, "The European Network on Neutron Techniques Standardization for Structural Integrity – NeT", in: Proceedings of ASME PVP 2008, Chicago, USA, July 27-31, 2008, ASME, CD Publication, 2008, Order No. I795CD, ISBN 0-7918-3828-5

6) M.C. Smith, A.C. Smith, R.C. Wimpory, C. Ohms,, Int. J. of Pressure Vessels and Piping, Vol. 120-121, Aug-Sep, 2014, pp. 93-140, DOI: 10.1016/j.ijpvp.2014.05.002

7) http://www.matterfp7.it/Layout/matter/index.asp

8) http://www.eera-jpnm.eu/

9) G. Barbieri, M. Cesaroni, L. Ciambella, G. Costanza, R. Montanari, La metallurgia Italiana, 107 (3) (2015) 37-45

10) L. Forest *et al.*, CEA Report DEN/DANS/DM2S/SEMT/LTA/NT/14-002/A (2014)

11) M. Hutchings, P. Withers, T. Holden, T. Lorentzen, *Introduction to the Characterization of Residual Stress by Neutron Diffraction*, Taylor & Francis, CRC Press, Boca Raton, London, New York, Singapore, 2005, ISBN 0-415

12) C. Ohms, R.V. Martins, O. Uca, A.G. Youtsos, P.J. Bouchard, M. Smith, M. Keavey, S.K. Bate, P. Gilles, R.C. Wimpory, L. Edwards, *The European Network on Neutron Techniques Standardization for Structural Integrity – NeT*, in: Proceedings of ASME PVP 2008, Chicago, USA, July 27-31, 2008, ASME, CD Publication, 2008, Order No. I795CD, ISBN 0-7918-3828-5

13) M.C. Smith, A.C. Smith, R.C. Wimpory, C. Ohms, *A review of the NeT Task Group 1 residual stress measurement and analysis round robin on a single weld bead-on-plate specimen*, International Journal of Pressure Vessels and Piping, Vol. 120-121, Aug-Sep, 2014, pp. 93-140, DOI: 10.1016/j.ijpvp.2014.05.002

14) http://dx.doi.org/10.17815/jlsrf-2-126

Figure captions.

Fig. 1. Micro-hardness measurements as a function of the distance from the weld center in the P91 TIG weld before (blue) and after (red) PWHT.

Fig. 2. Optical micrography observation of P91 TIG weld.

Fig. 3. Comb-like un-strained reference sample for P91 TIG weld.

Fig. 4. 316L (N) LB – GMAW specimen as seen from the top (a) and SEM cross-sectional observation of the weld (b).

Fig. 5. Cross section picture of 316LN steel LB – GMAW weld (top) and comb-like unstrained reference sample (bottom).

Fig. 6. 2D stress mapping (X and Y axes defined as in Fig. 3) for P91 TIG weld: a) transverse stresses, b) normal stresses, c) longitudinal stresses measured at a depth of approximately 2 mm inside the weld.

Fig. 7. Stresses as a function of distance from the weld center along a line below the weld cap in the P91 TIG weld.

Fig. 8. Stresses as a function of the distance from the weld center in AISI316LN LB – GMAW along lines below weld cap (a), at mid-thickness (b), at weld root (c).

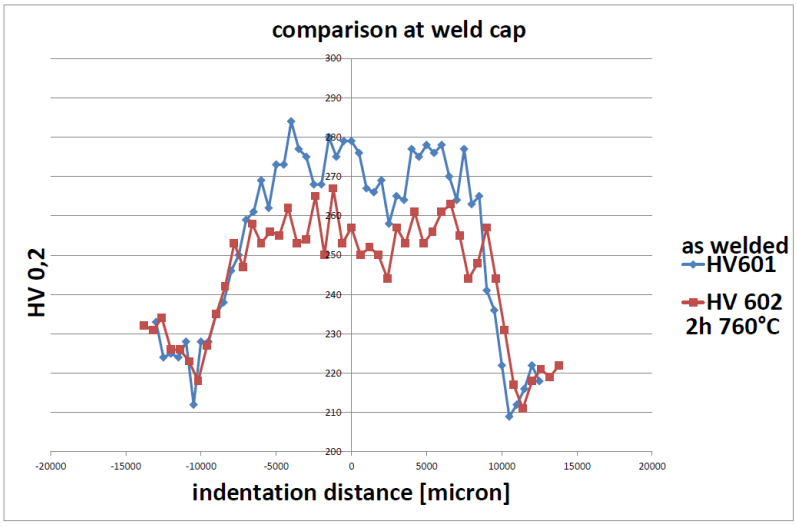

Fig. 1. Micro-hardness measurements as a function of the distance from the weld center in the P91 TIG weld before (blue) and after (red) PWHT.

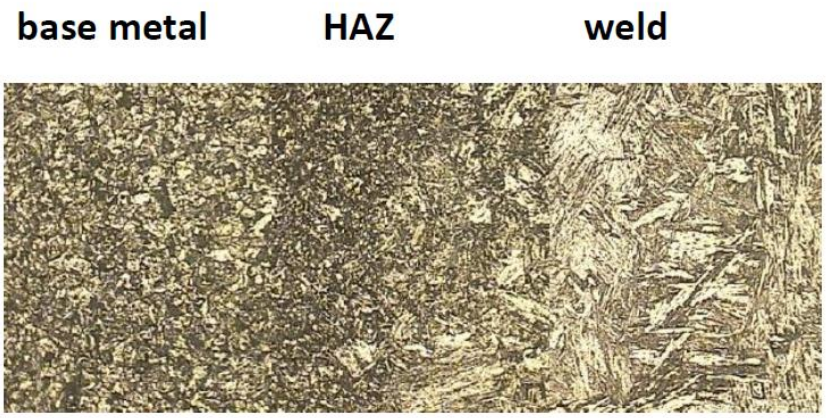

Fig. 2. Optical micrography observation of P91 TIG weld.

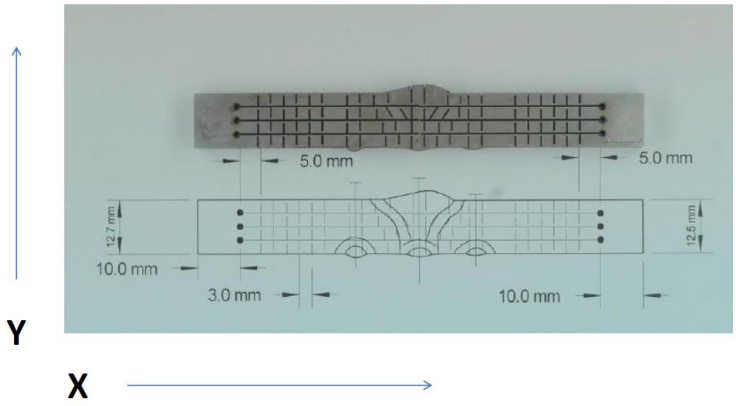

Fig. 3. Comb-like un-strained reference sample for P91 TIG weld.

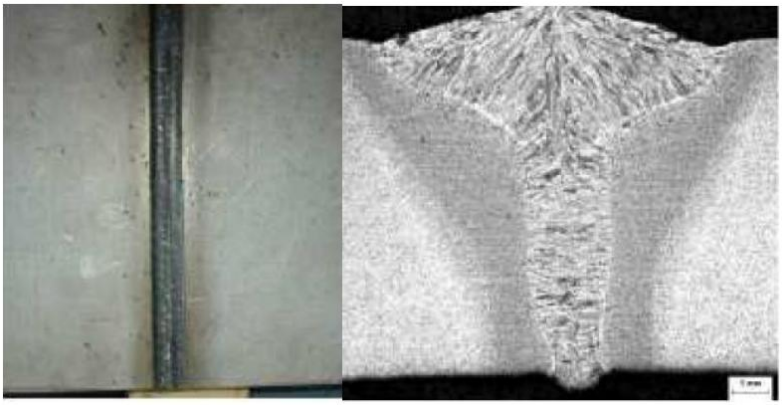

a) **b)**

Fig. 4. 316L (N) LB – GMAW specimen as seen from the top (a) and SEM cross-sectional observation of the weld (b).

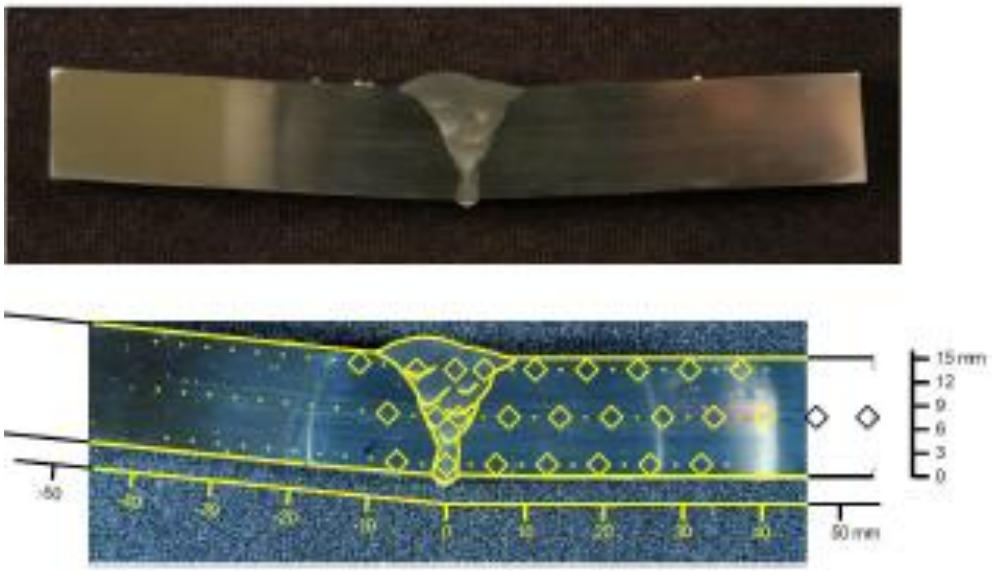

Fig. 5. Cross section picture of 316LN steel LB – GMAW weld (top) and comb-like unstrained reference sample (bottom).

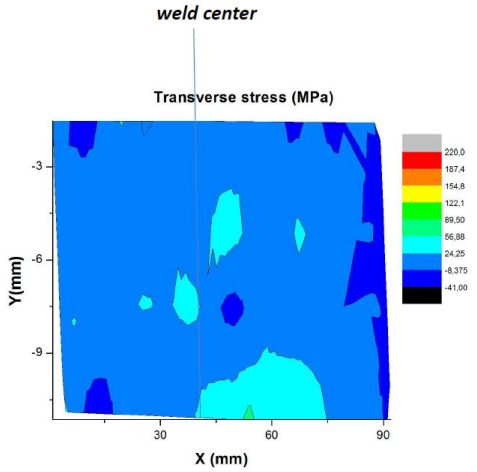

a)

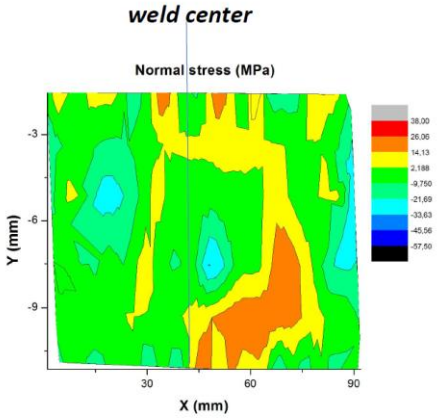

b)

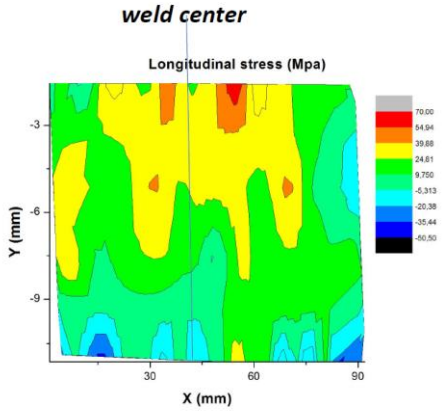

c)

Fig. 6. 2D stress mapping (X and Y axes defined as in Fig. 3) for P91 TIG weld: a) transverse stresses, b) normal stresses, c) longitudinal stresses measured at a depth of approximately 2 mm inside the weld.

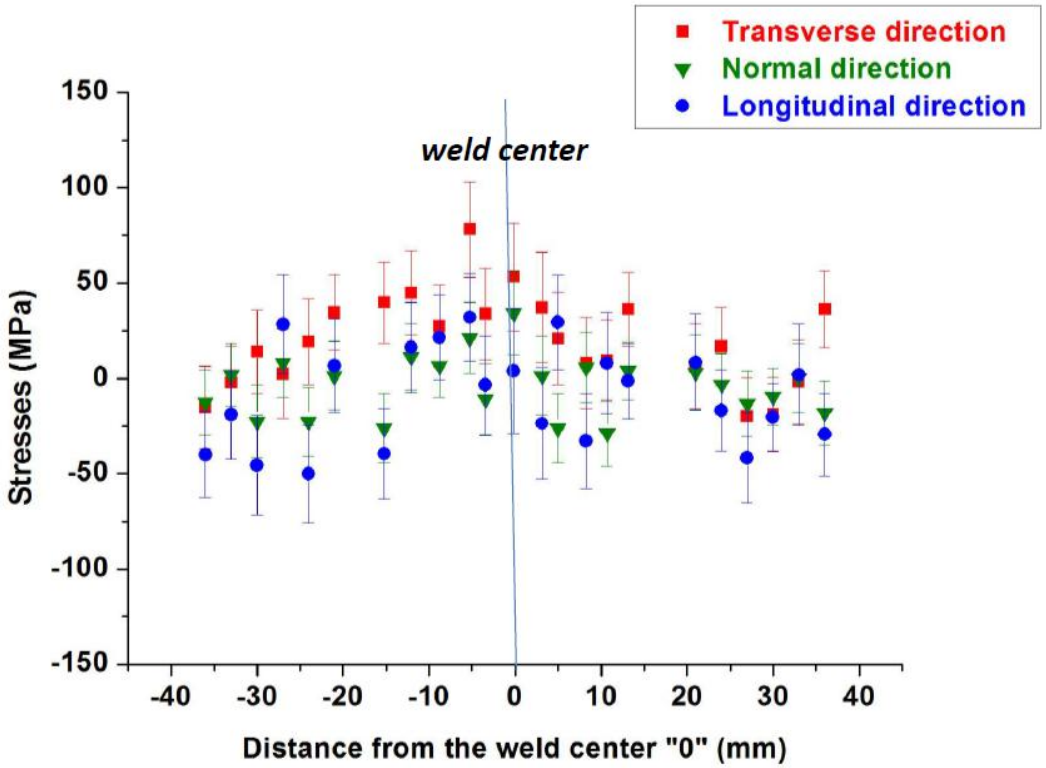

Fig. 7. Stresses as a function of distance from the weld center along a line below the weld cap in the P91 TIG weld.

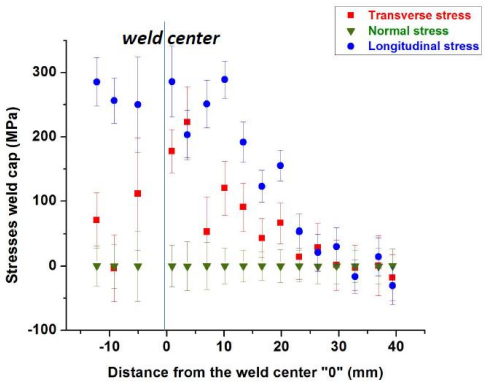

a)

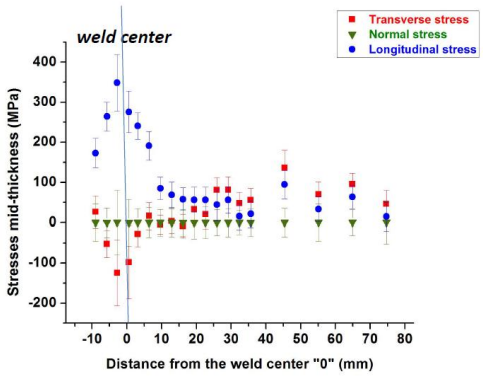

b)

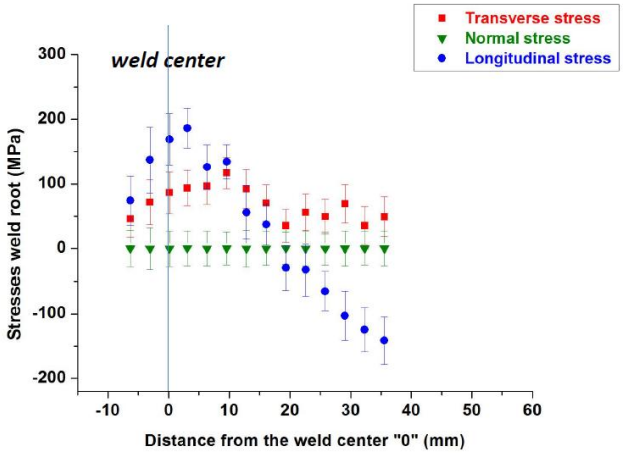

c)

Fig. 8. Stresses as a function of the distance from the weld center in AISI316LN LB – GMAW along lines below weld cap (a), at mid-thickness (b), at weld root (c).